Genetics in Medicine

Phenotypic spectrum and transcriptomic profile associated with germline variants in TRAF7

--Manuscript Draft--

Manuscript Number:	
Article Type:	Article
Section/Category:	Clinical Genetics and Genomics
Keywords:	TRAF7; craniofacial development; intellectual disability; blepharophimosis; patent ductus arteriosus
Corresponding Author:	Christopher Thomas Gordon, PhD Institut hospitalo-universitaire Imagine Institut des Maladies Genetiques PARIS, FRANCE
First Author:	Laura Castilla-Vallmanya
Order of Authors:	Laura Castilla-Vallmanya
	Kaja Selmer
	Clémantine Dimartino
	Raquel Rabionet
	Bernardo Blanco-Sánchez
	Sandra Yang
	Margot Reijnders
	Antonie van Essen
	Myriam Oufadem
	Magnus Vigeland
	Barbro Stadheim
	Gunnar Houge
	Helen Cox
	Helen Kingston
	Jill Clayton-Smith
	Jeffrey Innis
	Maria Iascone
	Anna Cereda
	Sara Gabbiadini
	Wendy Chung
	Victoria Sanders
	Joel Charrow
	Emily Bryant
	John Millichap
	Antonio Vitobello
	Christel Thauvin
	Frederic Tran Mau-Them
	Laurence Faivre

	Gaetan Lesca
	Audrey Labalme
	Christelle Rougeot
	Nicolas Chatron
	Damien Sanlaville
	Katherine Christensen
	Amelia Kirby
	Raymond Lewandowski
	Rachel Gannaway
	Maha Aly
	Anna Lehman
	Lorne Clarke
	Luitgard Graul-Neumann
	Christiane Zweier
	Davor Lessel
	Bernarda Lozic
	Ingvild Aukrust
	Ryan Peretz
	Robert Stratton
	Thomas Smol
	Anne Dieux-Coëslier
	Joanna Meira
	Elizabeth Wohler
	Nara Sobreira
	Erin Beaver
	Jennifer Heeley
	Lauren Briere
	Frances High
	David Sweetser
	Melissa Walker
	Catherine Keegan
	Parul Jayakar
	Marwan Shinawi
	Wilhelmina Kerstjens-Frederikse
	Dawn Earl
	Victoria Siu
	Emma Reesor
	Tony Yao
	Robert Hegele
	Olena Vaske
	Shannon Rego

	Kevin Shapiro
	Brian Wong
	Michael Gambello
	Marie McDonald
	Danielle Karlowicz
	Roberto Colombo
	Alessandro Serretti
	Lynn Pais
	Anne O'Donnell-Luria
	Alison Wray
	Simon Sadedin
	Belinda Chong
	Tiong Tan
	John Christodoulou
	Susan White
	Anne Slavotinek
	Deborah Barbouth
	Dayna Morel Swols
	Mélanie Parisot
	Christine Bole-Feysot
	Patrick Nitschké
	Véronique Pingault
	Arnold Munnich
	Megan Cho
	Valérie Cormier-Daire
	Susanna Balcells
	Stanislas Lyonnet
	Daniel Grinberg
	Jeanne Amiel
	Roser Urreizti
	Christopher Thomas Gordon, PhD
Manuscript Region of Origin:	FRANCE
Abstract:	Purpose Somatic variants in tumor necrosis factor receptor-associated factor 7 (TRAF7) cause meningioma and other cancers, while germline variants have recently been identified in seven patients with a syndrome associating cardiac, facial and digital anomalies with developmental delay. We aimed to define the clinical and mutational spectrum associated with TRAF7 germline variants through identification and description of 45 new patients, and to determine the effects of the variants at a molecular level through transcriptomic analysis of patient fibroblasts.Methods We performed exome, targeted capture and Sanger sequencing in a series of patients with undiagnosed developmental disorders. Phenotypic and mutational comparisons

	were facilitated through data exchange platforms. Whole transcriptome sequencing (RNA-Seq) was performed on RNA from patient- and control-derived fibroblasts.Results We identified heterozygous missense variants in TRAF7 as the cause of a developmental delay-malformation syndrome in 45 patients. Major features include a recognizable facial gestalt (characterized in particular by blepharophimosis), short neck, pectus carinatum, digital deviations and patent ductus arteriosus. Almost all variants occur in the WD40 repeats of TRAF7 and most are recurrent. Dysregulation of several genes, differentially-expressed in patient fibroblasts, plausibly contributes to the pathogenesis of the disorder.Conclusion We provide the first large-scale analysis of the clinical and mutational spectrum associated with the TRAF7 developmental syndrome, and we shed light on the molecular etiology of the disorder through transcriptome studies.

09 November 2019, Paris.

Dear Editor,

We would like to submit our manuscript entitled: "**Phenotypic spectrum and transcriptomic profile associated with germline variants in *TRAF7***" by Castilla-Vallmanya and co-workers for consideration as an Article to Genetics in Medicine.

Somatic variants in *TRAF7* are known to cause meningioma, while germline *TRAF7* variants have recently been identified in seven patients with a syndrome associating cardiac, facial and digital malformations with developmental delay/intellectual disability. In the submitted manuscript, we provide the first large-scale analysis of the clinical and mutational spectrum associated with the *TRAF7* developmental syndrome, through identification and description of 45 new patients. Major features include a recognizable facial gestalt (characterized in particular by blepharophimosis), short neck, pectus carinatum, digital deviations and patent ductus arteriosus. Almost all variants identified are *de novo* heterozygous missense, occurring in the WD40 repeats of TRAF7. Intriguingly, the somatic mutations previously reported in meningiomas also occur in the WD40 repeats, but are non-overlapping with the syndromic variants, suggesting different mechanisms of pathogenicity.

We also performed RNA-Seq of *TRAF7* syndrome patient fibroblasts, which led to the identification of several differentially-expressed genes, whose dysregulation plausibly contributes to the pathogenesis of the disorder.

Our findings will improve genetic counseling options and medical care strategies for patients with variants in *TRAF7* and will stimulate further investigation into the role of *TRAF7* in embryonic development.

All authors have read and approved the final version of the manuscript.

We have included a competing financial interests statement in the manuscript (two authors are employees of GeneDx, Inc.).

We have received and archived written consent for participation/publication from every individual whose data is included, including written consent to publish photographs (where applicable).

We hope you will consider our manuscript for publication in Genetics in Medicine and we look forward to hearing your response.

On behalf of all authors,

Yours sincerely,

Christopher Gordon (PhD), Institut Imagine, Paris, France.

Email: chris.gordon@inserm.fr

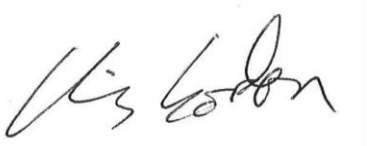

Phenotypic spectrum and transcriptomic profile associated with germline variants in *TRAF7*

Laura Castilla-Vallmanya, MSc[1], Kaja K. Selmer, MD, PhD[2,3], Clemantine Dimartino, MSc[4,5], Raquel Rabionet, PhD[1], Bernardo Blanco-Sánchez, PhD[4,5], Sandra Yang, MS, CGC[6], Margot R. F. Reijnders, MD, PhD[7], Antonie J. van Essen, MD, PhD[8,†], Myriam Oufadem, MSc[4,5], Magnus D. Vigeland, PhD[9,10], Barbro Stadheim, MD[9], Gunnar Houge, MD, PhD[11], Helen Cox, MD[12], Helen Kingston, MD[13,14], Jill Clayton-Smith, MD[13,14], Jeffrey W. Innis, MD, PhD[15], Maria Iascone, PhD[16], Anna Cereda, MD[16], Sara Gabbiadini, MD[16], Wendy K. Chung, MD, PhD[17], Victoria Sanders, MS, CGC[18,19], Joel Charrow, MD[18], Emily Bryant, MS, CGC[18], John Millichap, MD[18], Antonio Vitobello, PhD[20,21], Christel Thauvin, MD, PhD[20,22], Frederic Tran Mau-Them, MD[20,21], Laurence Faivre, MD, PhD[21,22], Gaetan Lesca MD[23,24], Audrey Labalme, MSc[23], Christelle Rougeot, MD[25], Nicolas Chatron, MD[23,24], Damien Sanlaville, MD, PhD[23,24], Katherine M. Christensen, MS, CGC[26], Amelia Kirby, MD[26], Raymond Lewandowski, MD[27], Rachel Gannaway, MS, CGC[27], Maha Aly, MSc[4,5], Anna Lehman, MD[28], Lorne Clarke, MD[28], Luitgard Graul-Neumann, MD[29], Christiane Zweier, MD, PhD[30], Davor Lessel, MD[31], Bernarda Lozic, MD, PhD[32], Ingvild Aukrust, PhD[11], Ryan Peretz, MD[33], Robert Stratton, MD[33], Thomas Smol, MD[34,35], Anne Dieux-Coëslier, MD[34], Joanna Meira, MD, MSc[36], Elizabeth Wohler, MS[37], Nara Sobreira, MD, PhD[37], Erin M. Beaver, MS, CGC[38], Jennifer Heeley, MD[38], Lauren C. Briere, MS, CGC[39], Frances A. High, MD, PhD[39], David A. Sweetser, MD, PhD[39], Melissa A. Walker, MD, PhD[40], Catherine E. Keegan, MD, PhD[15], Parul Jayakar, MD[41], Marwan Shinawi, MD[42], Wilhelmina S. Kerstjens-Frederikse, MD, PhD[8], Dawn L. Earl, ARNP[43], Victoria M. Siu, MD[44], Emma Reesor, BASc[44], Tony Yao, BMSc[44], Robert A. Hegele, MD[44], Olena M. Vaske, PhD[45], Shannon Rego, MS[46], Undiagnosed Diseases Network, Care4Rare Canada Consortium,

Kevin A. Shapiro, MD, PhD[47], Brian Wong, MD[47], Michael J. Gambello, MD, PhD[48], Marie McDonald, MD[49], Danielle Karlowicz, CGC[49], Roberto Colombo, PhD[50,51], Alessandro Serretti, MD[52], Lynn Pais, MS[53], Anne O'Donnell-Luria, MD, PhD[53], Alison Wray, MD[54], Simon Sadedin, PhD[55], Belinda Chong, PhD[55], Tiong Y. Tan, MBBS, PhD[55,56], John Christodoulou, MD, PhD[55,56], Susan M. White, MD[55,56], Anne Slavotinek, MBBS, PhD[57], Deborah Barbouth, MD[58], Dayna Morel Swols, MS, CGC[58], Mélanie Parisot, BTS[59,60], Christine Bole-Feysot, PhD[59,60], Patrick Nitschké, PhD[5,61], Véronique Pingault, PhD[4,5,62], Arnold Munnich, MD, PhD[5,62], Megan T. Cho, MSc, CGC[6], Valérie Cormier-Daire, MD, PhD[5,62,63], Susanna Balcells, PhD[1], Stanislas Lyonnet, MD, PhD[4,5,62], Daniel Grinberg, PhD[1], Jeanne Amiel, MD, PhD[4,5,62], Roser Urreizti, PhD[1,*], Christopher T. Gordon, PhD[4,5,*,#]

1. Department of Genetics, Microbiology and Statistics, Faculty of Biology, IBUB, Universitat de Barcelona; CIBERER, IRSJD, Barcelona, Spain.
2. Department of Research and Innovation, Division of Clinical Neuroscience, Oslo University Hospital and the University of Oslo, Oslo, Norway.
3. The National Center for Epilepsy, Oslo University Hospital, Oslo, Norway.
4. Laboratory of embryology and genetics of human malformations, Institut National de la Santé et de la Recherche Médicale (INSERM) UMR 1163, Institut Imagine, Paris, France.
5. Paris Descartes-Sorbonne Paris Cité University, Institut Imagine, Paris, France.
6. GeneDx, Gaithersburg, MD, USA.
7. Department of Clinical Genetics, Maastricht University Medical Center, Maastricht, The Netherlands.
8. Department of Genetics, University Medical Center Groningen, Groningen, The Netherlands.

9. Department of Medical Genetics, Oslo University Hospital, Oslo, Norway.
10. Institute of Clinical Medicine, University of Oslo, Norway.
11. Department of Medical Genetics, Haukeland University Hospital, Bergen, Norway.
12. West Midlands Regional Genetics Service, Birmingham Women's NHS Foundation Trust, Birmingham Women's Hospital, Edgbaston, Birmingham, UK.
13. Manchester Centre for Genomic Medicine, Central Manchester University Hospitals NHS Foundation Trust, Academic Health Sciences Centre, Manchester, UK.
14. Division of Evolution and Genomic Sciences, University of Manchester, School of Biological Sciences, Manchester, UK.
15. Departments of Human Genetics, Pediatrics and Internal Medicine, University of Michigan, Ann Arbor, MI, USA.
16. Department of Pediatrics, ASST Papa Giovanni XXIII, Bergamo, Italy.
17. Departments of Pediatrics and Medicine, Columbia University Medical Center, New York, NY, USA.
18. Ann & Robert H Lurie Children's Hospital of Chicago, Chicago, IL, USA.
19. Northwestern University Feinberg School of Medicine, Chicago, IL, USA.
20. UF Innovation en diagnostic genomique des maladies rares, CHU Dijon Bourgogne, Dijon, France.
21. INSERM UMR1231 GAD, Dijon, France.
22. Centre de Reference maladies rares “Anomalies du Developpement et syndrome malformatifs” de l’Est, Centre de Genetique, Hopital d’Enfants, FHU TRANSLAD, CHU Dijon Bourgogne, Dijon, France.
23. Department of Medical Genetics, Lyon Hospices Civils, Lyon, France.

24. Institut NeuroMyoGène, CNRS UMR 5310 - INSERM U1217, Université de Lyon, Université Claude Bernard Lyon 1, Lyon, France.
25. Hôpital Femme Mère Enfant, Service de Neuropédiatrie, Bron, France.
26. Saint Louis University School of Medicine, St. Louis, MO, USA.
27. Department of Human and Molecular Genetics, Virginia Commonwealth University, Richmond, VA, USA.
28. Department of Medical Genetics, The University of British Columbia, Vancouver, BC, Canada.
29. Institute of Human Genetics, Charité, Universitätsmedizin Berlin, Berlin, Germany.
30. Institute of Human Genetics, Friedrich-Alexander-Universität Erlangen-Nürnberg, Erlangen, Germany.
31. Institute of Human Genetics, University Medical Center Hamburg-Eppendorf, Hamburg, Germany.
32. Department of Pediatrics, University Hospital Centre Split; University of Split, School of medicine, Split, Croatia.
33. Driscoll Children's Hospital, Corpus Christi, TX, USA.
34. Institut de Génétique Médicale, CHU Lille, Lille, France.
35. Université de Lille, EA7364 RADEME, Lille, France.
36. Division of Medical Genetics, University Hospital Professor Edgard Santos/ Federal University of Bahia (UFBA), Salvador, Bahia, Brazil.
37. McKusick-Nathans Department of Genetic Medicine, Johns Hopkins University, Baltimore, MD, USA.
38. Mercy Kids Genetics, Mercy Children's Hospital, St. Louis, MO, USA.

39. Division of Medical Genetics & Metabolism, Massachusetts General Hospital *for* Children, Boston, MA, USA.
40. Department of Pediatric Neurology, Massachusetts General Hospital *for* Children, Boston, MA, USA.
41. Division of Genetics and Metabolism, Nicklaus Children's Hospital, Miami, FL, USA.
42. Department of Pediatrics, Division of Genetics and Genomic Medicine, Washington University School of Medicine, St. Louis, MO, USA.
43. Seattle Children's Hospital, Seattle, WA, USA.
44. University of Western Ontario, London, ON, Canada.
45. Department of Molecular, Cell and Developmental Biology, University of California Santa Cruz, Santa Cruz, CA, USA.
46. Institute for Human Genetics, University of California San Francisco, San Francisco, CA, USA.
47. Cortica Healthcare, San Diego, CA, USA.
48. Department of Human Genetics, Division of Medical Genetics, Emory University School of Medicine, Atlanta, GA, USA.
49. Division of Medical Genetics, Department of Pediatrics, Duke University Medical Center, Durham, NC, USA.
50. Faculty of Medicine, Catholic University, IRCCS Policlinico Gemelli, Rome, Italy.
51. Center for the Study of Rare Hereditary Diseases (CeSMER), Niguarda Ca' Granda Metropolitan Hospital, Milan, Italy.
52. Department of Biomedical and Neuromotor Sciences, University of Bologna, Bologna, Italy.

53. Broad Center for Mendelian Genomics, Program in Medical and Population Genetics, Broad Institute of Massachusetts Institute of Technology and Harvard, Cambridge, MA, USA.
54. Royal Children's Hospital, Melbourne, Australia.
55. Victorian Clinical Genetics Services, Murdoch Children's Research Institute, Melbourne, Australia.
56. Department of Paediatrics, University of Melbourne, Melbourne, Australia.
57. Department of Pediatrics, University of California San Francisco, San Francisco, CA, USA.
58. Dr John T. Macdonald Foundation Department of Human Genetics, University of Miami, Miller School of Medicine, Miami, FL, USA.
59. Genomics Core Facility, Institut Imagine-Structure Fédérative de Recherche Necker, INSERM UMR 1163, Paris, France.
60. INSERM US24/CNRS UMS3633, Paris Descartes-Sorbonne Paris Cité University, Paris, France.
61. Bioinformatics Platform, INSERM UMR 1163, Institut Imagine, Paris, France.
62. Département de Génétique, Hôpital Necker-Enfants Malades, Assistance Publique Hôpitaux de Paris, Paris, France.
63. Laboratory of Molecular and Physiopathological Bases of Osteochondrodysplasia, INSERM UMR 1163, Institut Imagine, Paris, France.

† deceased

* equal co-last

corresponding author: Email: chris.gordon@inserm.fr ; Tel: +33 1 42 75 43 08.

Abstract

Purpose: Somatic variants in tumor necrosis factor receptor-associated factor 7 (*TRAF7*) cause meningioma and other cancers, while germline variants have recently been identified in seven patients with a syndrome associating cardiac, facial and digital anomalies with developmental delay. We aimed to define the clinical and mutational spectrum associated with *TRAF7* germline variants through identification and description of 45 new patients, and to determine the effects of the variants at a molecular level through transcriptomic analysis of patient fibroblasts.

Methods: We performed exome, targeted capture and Sanger sequencing in a series of patients with undiagnosed developmental disorders. Phenotypic and mutational comparisons were facilitated through data exchange platforms. Whole transcriptome sequencing (RNA-Seq) was performed on RNA from patient- and control-derived fibroblasts.

Results: We identified heterozygous missense variants in *TRAF7* as the cause of a developmental delay-malformation syndrome in 45 patients. Major features include a recognizable facial gestalt (characterized in particular by blepharophimosis), short neck, pectus carinatum, digital deviations and patent ductus arteriosus. Almost all variants occur in the WD40 repeats of TRAF7 and most are recurrent. Dysregulation of several genes, differentially-expressed in patient fibroblasts, plausibly contributes to the pathogenesis of the disorder.

Conclusion: We provide the first large-scale analysis of the clinical and mutational spectrum associated with the *TRAF7* developmental syndrome, and we shed light on the molecular etiology of the disorder through transcriptome studies.

Keywords: *TRAF7*, craniofacial development, intellectual disability, blepharophimosis, patent ductus arteriosus.

Introduction

The tumor necrosis factor receptor (TNF-R)-associated factor (TRAF) family contains seven members defined by shared protein domains and their involvement in mediating signal transduction from TNF-R superfamily members.[1] TRAF7 contains an N-terminal RING finger domain, an adjacent TRAF-type zinc finger domain, a coiled-coil domain and seven C-terminal WD40 repeats (Figure 1). The WD40 repeats are unique to TRAF7 within the TRAF family, with all other members instead containing a C-terminal TRAF domain. *In vitro* studies have suggested that TRAF7 plays a role in the regulation of several transcription factors through various mechanisms. It participates in the signal transduction of cellular stress stimuli, such as TNFα stimulation, by activating pathways leading to increased transcriptional activity of AP1 and CHOP/gadd153.[2–4] These effects are thought to be mediated by synergy between TRAF7 and the MAP3 kinase MEKK3, leading to the phosphorylation of JNK and p38 (regulators of AP1 and CHOP), with interaction of TRAF7 and MEKK3 occurring via the TRAF7 WD40 repeats.[2,3] Depending on the context, TRAF7 can positively or negatively regulate the activity of NF-κB, through ubiquitination of pathway components p65 and NEMO.[2,5,6] It also ubiquitinates p53,[7] and the activity of the proto-oncogene c-Myb is negatively regulated by TRAF7 through sumoylation and consequent sequestering in the cytosol.[8] In endothelial cells, TRAF7 interacts with the C-terminus of ROBO4 to suppress hyperpermeability during inflammation.[9]

Somatic missense variants in *TRAF7*, concentrated within the WD40 domains and frequently recurrent, have been identified in meningiomas, mesotheliomas, intraneural perineuriomas and adenomatoid tumors of the genital tract.[10–17] Heterozygous germline variants in *TRAF7* have recently been reported in seven patients with a developmental disorder involving cardiac, facial,

and digital anomalies and developmental delay (OMIM #618164).[18] Here, we refine our understanding of the *TRAF7* mutational and phenotypic spectrum through the identification of 45 previously undescribed patients, and thereby define a syndrome with a recognizable facial gestalt, specific skeletal and cardiac defects, and developmental delay/intellectual disability, which we propose to name the *TRAF7* syndrome. Almost all identified variants fall in the WD40 repeats, most are recurrent and all are missense, suggestive of a gain-of-function or dominant negative mechanism, rather than haploinsufficiency. Intriguingly, somatic and germline variants do not overlap. We also present a transcriptomic analysis of fibroblasts from several patients, thereby providing insights into the pathways perturbed by *TRAF7* alteration.

Materials and Methods

Variant identification

Genetic testing was performed according to approved institutional ethical guidelines and consent was obtained from all families. Exome sequencing was performed in various centers worldwide, using standard approaches (details available upon request). Targeted capture sequencing of *TRAF7*, in a panel of genes implicated in craniofacial malformations, was performed during clinical diagnostic screening at the Necker Hospital, using a SureSelect kit (Agilent) for capture followed by sequencing on a HiSeq machine (Illumina). Polyphen-2[19] was used for predicting the pathogenicity of missense variants.

Cell culture

Fibroblasts were obtained from skin biopsies of four patients (age at biopsy range: 8 to 19 years) and six controls (age at biopsy range: 17 years to adult). Corresponding informed consent and

institutional ethics approval were obtained (Ethics Committee of the Universitat de Barcelona, IRB00003099), and all methods were performed in accordance with the relevant guidelines and regulations. Fibroblasts were cultured in DMEM supplemented with 10% FBS (Gibco, LifeTechnologies) and 1% penicillin-streptomycin (Gibco, LifeTechnologies) and were maintained at 37ºC and 5% CO_2. When appropriate, cells were treated with 10 ng/µl recombinant human TNFα protein (R&D systems) for 6, 24 or 48 hours.

Cell viability assay

Fibroblasts were plated in 96-well plates and synchronized through serum deprivation for 24 hours. Cell viability was tested using an MTT assay, with a solution of 0.5 mg/ml Thiazolyl Blue Tetrazolium Bromide (Sigma-Aldrich) in DMEM (Gibco, LifeTechnologies). After 4 hours, formazan crystals were dissolved using DMSO (Merck Millipore) and absorbance was read at 560 nm.

Total RNA isolation and cDNA retrotranscription

RNA was extracted from fibroblasts using the High Pure RNA Isolation Kit (Roche), following the manufacturer's instructions. Integrity and purity of the RNA was tested by agarose gel electrophoresis and 260/230 and 260/280 absorbance ratios using an ND-1000 Spectrophotometer (Nanodrop Technologies). All samples reached the quality and integrity standards for qRT-PCR. For RNA-Sequencing (RNA-Seq) analysis, the quality standards of half of the samples were tested on an Agilent Bioanalyzer 2100 (Agilent Technologies). RNA was retrotranscribed using the High-capacity cDNA Reverse Transcription kit (Applied Biosystems).

RNA-Sequencing and data analysis

RNA-Seq was performed by LEXOGEN, Inc. using the QuantSeq 3' mRNA-Seq FWD kit for library preparation. Single-end reads were aligned to the human reference genome (GRCh37/hg19) and transcriptome using the STAR aligner. Quality metrics were obtained with tools of the RSEQC Quality control package. Differential expression analysis was performed using the R package DESeq2. The threshold to be considered as a differentially expressed gene (DEG) was set at a false discovery rate (FDR) ≤ 0.05 and a $|\log_2 \text{fold change}| \geq 1$.

Real-time PCR

qPCR was performed using UPL probes (Roche), according to the manufacturer's instructions. For every assay, the efficiency (E) of the reaction was calculated from a 7 point standard curve. Genomic DNA contamination was assessed and not detected in the samples. Amplification was done using the thermocycler Light Cycler 480 (Roche). Each sample was run in triplicate and the relative transcription level was quantified with the Crossing Point cycle calculation using the Light Cycler® 480 Software (release 1.5.0) (Roche). The *GAPDH* and *PPIA* genes were used as reference genes as they displayed the minimum coefficient of variation. The primer sequences and UPL probes used are available on request.

Ingenuity pathway analysis

Ingenuity Pathway Analysis (IPA, Qiagen) was performed on genes that showed an FDR ≤ 0.1 and $|\log_2 \text{fold change}| \geq 0.38$. Separate runs were performed for each treatment condition. IPA uses the Fisher's Exact Test to calculate statistical significance, considering associations between DEGs and annotated sets of molecules, with a p-value <0.05 ($-\log_{10}$ p-value >1.3) considered to be non-random.

Results

Identification of pathogenic variants in *TRAF7*

We performed exome sequencing, targeted capture sequencing and Sanger sequencing on 45 individuals with undiagnosed, syndromic developmental delay/intellectual disability and dysmorphic facial features (Table S1). Comparison of phenotypes and variants was facilitated by the data exchange platforms GeneMatcher[20] and DECIPHER.[21] All 45 individuals harbored missense variants in *TRAF7*. The cohort includes 36 sporadic cases in which the *TRAF7* variant was *de novo*, one patient with low level maternal mosaicism for the *TRAF7* variant, five cases with unknown inheritance and one familial case (patients 24-26) in which affected dizygotic twins inherited a *TRAF7* variant from their affected mother, in whom the variant arose *de novo* (Figure S1). Almost all variants occurred in the WD40 repeats (Figure 1). Patients 1, 2 and 4 are sporadic cases carrying *TRAF7* variants of unknown inheritance in the coiled-coil domain, and display phenotypes only partly overlapping those frequently observed in the rest of the cohort (further details below). We therefore consider these three individuals as having *TRAF7* variants of unknown significance. None of the variants present in patients 1-45 have been reported in the Genome Aggregation Database (gnomAD, dataset v2.1). All affect highly conserved amino acids (based on Multiz alignments of 100 vertebrates at the UCSC Genome Browser) and all (except one coiled-coil variant) are predicted possibly or probably damaging by Polyphen-2 (Table S2). The variants in the 45 patients occur at 20 amino acid positions (Figure 1); recurrent variants occur on eight of these, with the most recurrent by far being p.(Arg655Gln) (13 index cases). The remaining recurrent variants each occur in two to four index cases, and different variants of the same residue are observed at two positions (p.(Ser558Phe) or p.(Ser558Tyr); p.(Phe617Leu) or

p.(Phe617Ser)). The finding of recurrent missense variants largely restricted to the WD40 repeats suggests a disease mechanism involving specific functional changes to the mutant TRAF7 protein, rather than haploinsufficiency. In gnomAD, *TRAF7* has a low probability of being loss-of-function intolerant (pLI = 0.02), further suggesting haploinsufficiency of *TRAF7* does not cause severe pediatric disease.

Phenotype associated with *TRAF7* variants

Clinical details of all patients are provided in Table S1, and a summary of the phenotypes in the core cohort of 42 patients (i.e., excluding the three patients with coiled-coil variants of unknown significance) is provided in Table S3. Many patients presented with feeding difficulties (n=24), often requiring tube feeding in infancy. Short stature was noted in 12 cases, low weight in five and microcephaly or macrocephaly in a total of 10. All patients had some form of developmental delay; intellectual disability (n=23) and/or speech delay (n=29) occurred in all but a small minority, while motor delay occurred in the majority (n=30). Hypotonia was noted in 17 patients. Autism spectrum disorder was observed in six cases and epilepsy in seven. There was a range of nonspecific anomalies on brain MRI (most frequently, enlarged ventricles). Almost all patients presented with anomalies of the palpebral fissures; most frequently blepharophimosis (n=33), along with epicanthus (n=20), telecanthus (n=14), ptosis (n=19) and up- or downslanting palpebral fissures (n=11) (Figure 2). Hypertelorism was reported in 17 cases. Ear anomalies (n=27) most frequently consisted of low-set, posteriorly rotated and/or protruding ears. Other frequent facial features include a bulbous nasal tip (n=17), wide or flat nasal bridge (n=11), micro- or retrognathia, albeit typically mild (n=13) and a high or prominent forehead (n=11). A computational composite from multiple patient photos further highlights the facial gestalt of the syndrome (Figure S2). Other skull shape anomalies, such as trigonocephaly, dolicocephaly,

plagiocephaly, brachycephaly or bitemporal narrowing, occurred in 18 cases, and craniosynostosis in three. Palatal anomalies (n=15) included submucous cleft and velopharyngeal insufficiency. Most patients presented with abnormalities of the extremities (Figure 3A). Although highly variable in nature, major anomalies of the hands were finger deviations (n=10), camptodactyly (n=10), brachydactyly (n=6) and syndactyly (n=5), and of the feet, overlapping toes (n=10), pes planus (n=10), varus or valgus abnormalities (n=10) and sandal gap (n=5). Joint limitation in the limbs, hypermobility and dislocations were occasionally present. Anomalies of the axial skeleton were frequent: short neck (n=24), pectus carinatum (n=17) and other chest shape anomalies (n=10, including barrel-shaped or narrow chest), rib anomalies (n=5), deviations of the vertebral column (n=7) and vertebral anomalies (n=14). Regarding the latter, cervical stenosis or spinal cord compression was of clinical concern in several cases. Congenital cardiac defects were also frequent: 24 patients had patent ductus arteriosus (many of which required surgical repair), nine had atrial and six had ventricular septal defects and 10 had anomalies of valves. Conductive and/or sensorineural hearing loss occurred in 21 cases. Anomalies of the eyes included refractive errors (n=10) and strabismus (n=10). Infrequent phenotypes included a range of kidney anomalies (n=10), cryptorchidism (n=7), hernias (n=11), inverted nipples (n=6) and lower limb edema (n=3). In addition to a similar facial appearance amongst many of the patients, other features contributed to an upper-body gestalt in several, i.e., short neck with sloping shoulders, pectus carinatum and relative macrocephaly (Figure 3B). Finally, amongst the few adult patients in our cohort (seven over 18 years), clinical signs of premature ageing[22] were noted - two women (20 years and 44 years) had progressive hair loss, the latter also had premature atherosclerosis, and a 26 year old male had premature osteoporosis and hair loss.

Amongst the differential diagnoses in our cohort, an Ohdo-related syndrome (OMIM 249620) was suspected in several patients, with *KAT6B* sequencing performed for five individuals prior to exome, highlighting that the *TRAF7* syndrome overlaps with the group of blepharophimosis-mental retardation syndromes[23]. Also, Noonan/RAS-MAPK pathway gene panels were tested in eight patients, suggesting similarities to rasopathies. Although almost all *TRAF7* variants were identified through trio exome sequencing, inclusion of *TRAF7* on an NGS panel of genes mutated in neurocristopathy and craniofacial malformation syndromes led to the identification of two further individuals through diagnostic screening (patients 5 and 29). In patients 38 and 42, a strong clinical suspicion of *TRAF7* syndrome, based on comparison with our cohort at the time, led to identification of a *TRAF7* variant through Sanger sequencing or reanalysis of a previously unresolved singleton exome, respectively, highlighting the recognizability of this syndrome.

As noted above, three individuals (1, 2 and 4) harbored variants of unknown inheritance in the coiled-coil domain of TRAF7 (pink variants in Figure 1). These patients presented with neurodevelopmental defects, with seizures in two. Their facial features were not reminiscent of those of patients with variants in the WD40 repeats. Interestingly, patient 3, the only case with a *de novo* coiled-coil variant, had typical *TRAF7* syndrome facial features (photographs were reviewed but permission to publish was denied). Of note, patient 4 had an endometrioid adenocarcinoma, diagnosed at 36 years.

Syndromic *TRAF7* missense variants affect gene expression

As a first approach to understand the effects of syndromic *TRAF7* missense variants, the expression of 17 genes was assessed by qRT-PCR using skin fibroblast RNA from three patients bearing different variants in the WD40 repeats [p.(Leu402Val), p.(Leu519Phe), p.(Arg655Gln);

patient numbers 6, 13, 33, respectively] versus fibroblast RNA from six control individuals. Of these, 9 genes (*EEF1A2, FLNB, IGFBP4, IGFBP7, LASS2, MMP2, NFKBIA, NOTCH3, SQSTM1*) were selected because their expression appeared to be altered in a previous global transcriptome analysis performed in *TRAF7*-silenced cells,[6] and because of their known involvement in human developmental disorders or putative role in developmental events relevant to the *TRAF7* syndrome. The expression of *JUN* (encoding a subunit of the AP1 transcription factor) was tested because although AP1 activity can be stimulated by TRAF7, the effect of TRAF7 on transcription of AP1 components is unknown. *TRAF7* itself was tested for auto-regulation. The rest are known NF-κB target genes (*CFLAR* (*cFLIP*), *CCL2* (*MCP1*), *VEGFA, MYC, BCL2, PTGS2* (*COX2*)).[24] The above genes were also tested after TNFα stimulation.

We found *NOTCH3* (ENSG00000074181) expression decreased by half in untreated patient cells (Figure 4), matching the direction of differential expression reported in *TRAF7*-silenced cells. In contrast, two other genes displayed an expression profile in patients opposite to that observed in *TRAF7*-silenced cells: *FLNB* (ENSG00000136068) expression levels in patients were over 2-fold higher than in controls, whereas *IGFBP7* (ENSG00000163453) RNA was 4-fold lower in patients. We also found differences in *BCL2* (ENSG00000171791), with lower expression levels in untreated patient cells than in controls, and *PTGS2* (ENSG00000073756), whose expression was reduced to one third in untreated patient cells. Regarding *TRAF7* itself, none of the three heterozygous missense variants tested altered its expression levels. In the same way, *JUN, EEF1A2, IGFBP4, NFKBIA, LASS2, MMP2, SQSTM1, CFLAR, CCL2, VEGFA* and *MYC* did not show any variation in their expression levels between patients and controls (data not shown).

To further characterize the effects that syndromic *TRAF7* missense variants could have on gene expression levels, we performed an mRNA transcriptomic analysis of skin fibroblasts. We used

samples from the three patients and the six controls, with and without TNFα treatment. We considered DEGs as presenting an adjusted p-value <0.05 and |log_2 fold change| in expression ≥1 (Table S4). We identified 76 DEGs in basal conditions (51.31% up-regulated and 48.68% down-regulated) and 90 DEGs after TNFα treatment (40% up-regulated and 60% down-regulated) (Figure 5A-5B). A substantial overlap in several DEGs was detected between the untreated and treated conditions, as 16 DEGs were up-regulated and 19 down-regulated independently of treatment (Figure 5C). In addition, 55 DEGs were identified only in the treatment condition, suggesting that *TRAF7* syndromic variants may cause an alteration of the signaling pathway that is activated as a response to TNFα ligand. Table 1 summarizes the top 10 up- and down-regulated genes.

Twelve DEGs were selected for qRT-PCR validation based on their high log_2 fold change and/or functional criteria (i.e., for most, involvement in a human developmental disorder or relevant phenotype in an animal model – see Discussion for details) (Table S5). For this step, an additional patient [number 36, bearing the variant p.(Arg655Gln)] was included. Results for seven out of the 12 were confirmatory (*ANGPT1*, *CASK*, *KIF26B*, *WNT5A*, *CFD*, *GPC6*, *KAZALD1*) (Figure 4B). *KRAS*, which was slightly upregulated in the RNA-Seq analysis, appeared downregulated in treated patient cells by qRT-PCR, while *RIT1* was slightly downregulated only in untreated cells by RNA-Seq and only in treated cells by qRT-PCR. Finally, three genes (*FOXP1*, *SPTAN1*, *MAPK11*) whose log_2 fold changes and significance values were below the general threshold to be considered as DEGs, but which had been selected based on functional criteria, were not validated.

To explore the different pathways and biological functions that might be affected, we performed IPA on the 726 DEGs identified under basal conditions using less stringent criteria than the preceding analyses (Table S6). The "Axonal guidance signaling" canonical pathway was

significantly enriched, as 26 genes within this pathway showed alterations in transcript levels between patients and controls. Other significantly enriched canonical pathways included "Wnt/Ca^{2+} pathway" and "Role of NFAT in Cardiac Hypertrophy" (Figure 5D). IPA results also showed significant enrichment amongst the DEGs for genes involved in the development and function of the cardiovascular and nervous systems (Figure 5E). Similar results were obtained under TNFα-treated conditions (data not shown).

Syndromic *TRAF7* missense variants have mild effects on cell viability

Putative differences in cell viability between patient and control fibroblasts were assessed, both in untreated and TNFα-treated conditions, during 24 or 48 hours. Although a slight tendency for increased cell viability was observed in patient fibroblasts under all conditions, significant differences were only observed at 24 hours of treatment with TNFα (Figure S3).

Discussion

In the present study, we have characterized the clinical features associated with germline variants in *TRAF7*, through analysis of 45 patients. In a cohort of seven patients, Tokita *et al* reported speech and motor delay, a range of dysmorphic facial features (including epicanthal folds, ptosis and dysmorphic ears), variable cardiac defects and anomalies of the extremities (digit deviations and variant creases) as principal phenotypes associated with *TRAF7* variants.[18] The large size of the cohort described here allowed us to further refine the phenotypic spectrum and to highlight several major phenotypes which were not emphasized previously: blepharophimosis, short neck, pectus carinatum and other thoracic defects, vertebral anomalies, patent ductus arteriosus and hearing loss. All the *TRAF7* variants in our cohort are missense and several are recurrent, with

one major mutational hotspot; p.(Arg655Gln). Previously, Tokita *et al* reported *TRAF7* variants at only four positions (also missense); two in the coiled-coil domain and two in the WD40 repeats (including p.(Arg655Gln)).[18] Our results reveal a highly skewed variant distribution along the protein, that was not evident in the prior study (Figure 1), and strongly implicate alteration of the WD40 repeats as the central disease mechanism.

The germline *TRAF7* variants reported here are strikingly mutually exclusive to the somatic variants previously identified in tumors (lower part of Figure 1). This is underscored by the presence of recurrent variants restricted to each disease; p.(Arg655Gln) identified in 13 index cases here but never previously reported in a tumor, and variants at Asn520 reported 39 times in meningioma[11,12] but not in syndromic patients. This suggests differences in activity of the mutant protein in each disease (for example, disruption of different protein-protein interactions or differences in degree of the same activity). Interestingly, even amongst somatic variants, there may also be a trend for certain variants to be more frequent in particular tumor types; p.(His521Arg) and p.(Ser561Arg) (in blue in Figure 1) are highly recurrent in adenomatoid tumors of the genital tract,[16] but have not been reported in meningiomas.[10–13] In a few cases, the same amino acid is mutated to a different residue in each disease; for example, the syndromic variant p.(Leu519Phe) and the meningioma variants p.(Leu519Pro) and p.(Leu519Arg) (the latter two are not included in Figure 1). To the best of our knowledge, there is only one syndromic variant, p.(Arg524Trp) (*de novo* or maternal mosaic in four unrelated cases here) that has also been reported in a tumor sample.[11] However, this meningioma also harbored a *SMO* variant, p.(Ala459Val), known to cause increased activity of SMO;[25] the oncogenicity of the *TRAF7* variant in this case is therefore unclear. One patient in our series with a variant of unknown significance in the coiled-coil domain had an endometrioid adenocarcinoma, while no tumors

were reported in the patients with variants in the WD40 domain (although only a few are adults). One patient (43 years of age) in the cohort of Tokita *et al*[18] had a meningioma. Meningiomas harboring a *TRAF7* variant typically also contain a variant in *KLF4, AKT1* or *PIK3CA*,[10–13] suggesting a second hit may be required for development of *TRAF7*-associated tumors. Careful monitoring of aging syndromic patients will be required in order to determine whether they have a greater risk of developing tumors.

WD40 repeats are typically protein- or nucleic acid-interaction surfaces,[26] and the WD40 domain of TRAF7 is known to interact with MEKK3[2,3] and with the DNA-binding domain of c-Myb.[8] Whether alteration of these or other interactions underlies *TRAF7* syndrome is unknown. Interestingly, *Mekk3* is required for early cardiovascular development in mice.[27] Also, phosphorylation of ERK1/2, which are MAP kinases downstream of MEKK3, is reduced in cells overexpressing *TRAF7* syndromic variants,[18] and loss of *Erk2* in mice causes craniofacial and cardiac malformations and neurogenesis defects.[28,29] *In vitro* overexpression of *TRAF7* harboring WD40 domain variants identified in adenomatoid tumors of the genital tract leads to activation of the NF-κB pathway,[16] and although dysregulation of this pathway has not typically been associated with congenital malformations in humans,[30] knock-out of *Ikka* (a central component of the NF-κB pathway) in mice results in craniofacial and skeletal defects.[31] The *TRAF7* mutation distribution identified here, with clustering of recurrent missense variants in the WD40 repeats, is more consistent with a gain-of-function or dominant negative effect rather than haploinsufficiency. Structural studies suggest TRAF proteins can form trimers via the coiled-coil domain,[32] and co-immunoprecipitation experiments have shown that TRAF7 can interact with itself[2] and with TRAF6.[33] An interesting possibility is that TRAF7 harboring syndromic variants

could dominantly interfere not only with wildtype TRAF7 molecules but also with other TRAF proteins during development. *TRAF7* loss of function animal models have not been reported. Amongst *TRAF* family members, *Traf4* knock-out mice have congenital malformation phenotypes, including tracheal ring disruption, spina bifida and axial skeletal defects;[34,35] the latter is of particular interest given the high frequency of costo-sternal and vertebral anomalies in *TRAF7* syndrome patients.

Tokita *et al* reported two *TRAF7* syndrome patients with variants in the coiled-coil domain (p.(Lys346Glu) and p.(Arg371Gly)), although these had no or less negative effect on ERK1/2 phosphorylation compared to the two WD40 repeat variants they identified (p.(Thr601Ala) and p.(Arg655Gln)). We report four individuals with coiled-coil domain variants, of which only one was confirmed to have a facial gestalt similar to patients with WD40 repeat variants. This suggests that some coiled-coil domain variants can have a similar molecular effect as those that perturb the WD40 domain. On the other hand, it has been reported that the coiled-coil domain of TRAF7 is required for interaction with NEMO,[6] and in combination with the zinc finger domain for homodimerization and subcellular localization,[2] raising the possibility that the molecular consequences of some coiled-coil domain variants may be different from those in the WD40 repeats. Confirmation of the causality of all *TRAF7* coiled-coil domain variants, and the associated phenotypic spectrum, will require further functional studies and analysis of a larger number of individuals in this mutational subset.

To gain a better understanding of the pathogenic role of syndromic *TRAF7* variants, patient fibroblasts were compared with controls at a transcriptomic level. As a first approach, 17 genes were selected and analyzed by qPCR. Nine of these genes had been found to be altered in

TRAF7-silenced cells in previous studies.[6] From these nine, only three showed differential expression in fibroblasts bearing *TRAF7* syndromic variants compared to controls. In particular, *FLNB* was significantly increased in patients compared to controls (over 2-fold) independently of the treatment, as opposed to *TRAF7* knock-down, which has been shown to lead to a reduction of *FLNB* expression.[6] FLNB is an actin-binding protein that regulates dynamic changes of the cytoskeleton and has essential scaffolding functions. Given the skeletal malformations present in patients with *TRAF7* variants, it is interesting that alterations in *FLNB* cause several skeletal dysplasias, including spondylocarpotarsal synostosis syndrome (OMIM #272460), Larsen syndrome (OMIM #150250), atelosteogenesis types I (OMIM #108720) and III (OMIM #108721) and boomerang dysplasia (OMIM #112310).[36] *IGFBP7* (also known as angiomodulin) was, on the other hand, underexpressed in patient fibroblasts independently of the treatment, while it was found overexpressed in *TRAF7*-depleted cells.[6] It is a matrix-bound factor, with knockdown causing vascular patterning defects in zebrafish[37] or inhibition of cardiogenesis in embryonic stem cells.[38] A homozygous variant in humans causes retinal arterial macroaneurysm with supravalvular pulmonic stenosis (OMIM #614224).[39] Reduced expression of *IGFBP7* may contribute to the cardiovascular defects in *TRAF7* syndrome patients. *TRAF7* syndrome patient fibroblasts also expressed lower levels of *NOTCH3*. *Notch3* knockout mice have defects in arterial differentiation and vascular smooth muscle cell maturation.[40] Toxic neomorphic variants in *NOTCH3* cause the cerebral arteriopathy CADASIL (OMIM #125310),[41] while C-terminal truncating variants cause lateral meningocele syndrome (OMIM #130720), which includes craniofacial, skeletal and cardiac defects that partly overlap with those of the *TRAF7* syndrome.[42] Given that the direction of gene expression changes in patient cells versus *TRAF7*-silenced cells can be divergent (*FLNB, IGFBP7*), the same (*NOTCH3*) or unchanged in patients, it is difficult to conclude on the basis of these experiments whether the *TRAF7* variants are more likely gain or

loss of function. The differences could stem from the cell types studied; previous studies on *TRAF7*-silencing were performed in an immortalized cell line[6] while we have analyzed primary fibroblasts.

Six other genes tested are downstream targets of NF-κB and are involved in processes such as inflammation, tumorigenesis and negative regulation of apoptosis.[24] From these, two genes showed significantly reduced expression in patient fibroblasts, namely *BCL2* and *PTGS2*. BCL2 is an anti-apoptotic factor that is deregulated in several human cancers.[43] *PTGS2* encodes COX2, which catalyzes the formation of the prostaglandin precursor PGH2 and is generally considered as an inflammation mediator.[44] The expression of *PTGS2* was reduced to one third in the patient fibroblasts without TNFα treatment. Interestingly, COX2 deficiency has been associated with inefficient closure of the ductus arteriosus in mice[45] and we observed patent ductus arteriosus in the majority of *TRAF7* syndrome patients, suggesting a pathogenic effect of COX2 deficiency in this context.

To further characterize the gene expression landscape in patients bearing syndromic *TRAF7* variants, we performed RNA-Seq of skin fibroblasts. Consistent with previous data suggesting that TRAF7 modulates the activity of several transcription factors, the expression of many genes was affected in patient cells. Pathway enrichment analysis of the identified DEGs highlighted pathways involved in the development and function of the nervous system, which could partly explain the intellectual disability present in patients harboring *TRAF7* variants. Interestingly, the cardiovascular system category was also enriched for DEGs; congenital heart defects are frequent in *TRAF7* syndrome patients. Several DEGs are especially interesting due to the role they play in

specific cellular processes and the effects that their alteration can produce. *ANGPT1*, *WNT5A* and *KIF26B* were the most downregulated genes in patient fibroblasts under basal conditions. *ANGPT1* encodes angiopoeitin 1 and homozygous knock-out in mice leads to severe vascular malformations and embryonic lethality.[46] Conditional knock-outs in mice have shown roles for *Angpt1* in cardiac morphogenesis[47,48] and its deregulation may contribute to the cardiovascular anomalies observed in our cohort. *Wnt5a* is required for the outgrowth of limbs and craniofacial and genital structures in mice,[49] and variants in *WNT5A* cause autosomal dominant Robinow syndrome (OMIM #180700), a condition which shares some skeletal features with the patients we report here.[50] *KIF26B* encodes a kinesin required for kidney development in mice,[51] and interestingly, together with WNT5A and ROR, it shapes a crucial noncanonical WNT pathway, especially relevant in cell migration events during embryogenesis.[52] *CASK*, mildly downregulated in the patients, encodes a synaptic scaffolding protein. Loss of function variants in this gene are responsible for an X-linked syndrome associating intellectual disability, microcephaly and pontine and cerebellar hypoplasia (OMIM #300749).[53] *GPC6*, *KAZALD1* and *CFD* were among the most upregulated genes in *TRAF7* syndrome patient fibroblasts. *GPC6* encodes a member of the glypican family of cell-surface heparan sulfate proteoglycans, and *GPC6* variants are responsible for a rare autosomal recessive condition defined by proximally shortened limbs; omodysplasia (OMIM #258315).[54] *KAZALD1* (also known as *IGFPB-rP10*) is expressed specifically in ossification regions of the head in mice and can promote osteoblast proliferation;[55,56] *KAZALD1* overexpression could therefore play a role in the craniofacial shape anomalies observed in *TRAF7* syndrome patients. *CFD* encodes the complement factor D, a serine protease that acts in the alternative complement pathway. In humans, factor D deficiency leads to an immunologic condition with susceptibility to bacterial infections.[57] The significance of *CFD* upregulation in *TRAF7* syndrome patient cells is unclear.

In conclusion, through analysis of a large series of patients, we have defined the phenotypic spectrum associated with germline *TRAF7* variants. The major features in our series are intellectual disability, motor delay, a recognizable facial gestalt including blepharophimosis, short neck, pectus carinatum, digital deviations, hearing loss and patent ductus arteriosus. *TRAF7* syndrome patients typically require assisted learning and may be at risk of cervical stenosis. Older patients may benefit from monitoring for development of premature ageing phenotypes and tumors, although at this stage we cannot conclude whether there is an increased risk of the latter. We have shown there is a strong bias for *TRAF7* syndrome-associated variants to occur in the WD40 repeats, and a major avenue for future investigation will involve determining whether there are different consequences on direction or strength of downstream signaling between these germline variants versus those previously reported in various cancers. Our transcriptomic studies of *TRAF7* syndrome patient fibroblasts revealed a large number of DEGs. The fact that the expression of some genes (but not all) is only affected after TNFα treatment indicates that TRAF7 function in this pathway is disturbed, but that this is not the only pathway affected by the syndromic variants. Several identified DEGs are involved in cardiovascular, skeletal or nervous system development or function, and are therefore relevant to the phenotypes observed in the patients. Further exploration of the link between *TRAF7* and these putative transcriptional targets is warranted in an animal model of the *TRAF7* syndrome.

Acknowledgements

We thank the families for their participation. This work was supported by the Agence Nationale de la Recherche (CranioRespiro project and “Investissements d’avenir” program (ANR-10-IAHU-01)) and MSD Avenir (Devo-Decode project). J.W.I. is supported by the Morton S. and Henrietta K. Sellner Professorship in Human Genetics. W.K.C. received grant support from the JPB Foundation and the Simons Foundation SFARI program. D.L. is supported by the German Research Foundation (DFG; LE 4223/1). The CAUSES Study was funded by the BC Children’s Hospital Foundation and Genome BC; investigators include Shelin Adam, Christele Du Souich, Alison Elliott, Anna Lehman, Jill Mwenifumbo, Tanya Nelson, Clara Van Karnebeek, and Jan Friedman. M.I. and A.C. were supported by the PG23 / FROM 2017 Call for Independent Research as part of the Rapid Analysis for Rapid carE (RARE) project. We thank Peedikayil Thomas, Mark Russell, Sarah Geisler, Jordan Shavit and Steven Grzegorski for helpful comments and efforts to explore *TRAF7* variant pathogenesis. The research conducted at the Murdoch Children’s Research Institute was supported by the Victorian Government's Operational Infrastructure Support Program. Sequencing and analysis provided by the Broad Institute of MIT and Harvard Center for Mendelian Genomics was funded by the National Human Genome Research Institute, the National Eye Institute, and the National Heart, Lung and Blood Institute (grant UM1 HG008900 to Daniel MacArthur and Heidi Rehm). The DDD study presents independent research commissioned by the Health Innovation Challenge Fund (grant number HICF-1009-003). This study makes use of DECIPHER (http://decipher.sanger.ac.uk), which is funded by the Wellcome. See ref[58] or www.ddduk.org/access.html for full acknowledgement. Support was also provided by the NIH National Human Genome Research Institute (award numbers U01HG009599 and UM1 HG006542) and an NIH Common Fund grant (U01HG00769). The content is solely the responsibility of the authors and does not necessarily represent the official views of the NIH[59].

Disclosure

M.T.C. and S.Y. are employees of GeneDx, Inc.

References

1. Zotti T, Scudiero I, Vito P, Stilo R. The Emerging Role of TRAF7 in Tumor Development. *J Cell Physiol*. 2017;232(6):1233-1238.
2. Bouwmeester T, Bauch A, Ruffner H, et al. A physical and functional map of the human TNF-alpha/NF-kappa B signal transduction pathway. *Nat Cell Biol*. 2004;6(2):97-105.
3. Xu L-G, Li L-Y, Shu H-B. TRAF7 potentiates MEKK3-induced AP1 and CHOP activation and induces apoptosis. *J Biol Chem*. 2004;279(17):17278-17282.
4. Scudiero I, Zotti T, Ferravante A, et al. Tumor necrosis factor (TNF) receptor-associated factor 7 is required for TNFα-induced Jun NH2-terminal kinase activation and promotes cell death by regulating polyubiquitination and lysosomal degradation of c-FLIP protein. *J Biol Chem*. 2012;287(8):6053-6061.
5. Tsikitis M, Acosta-Alvear D, Blais A, et al. Traf7, a MyoD1 transcriptional target, regulates nuclear factor-κB activity during myogenesis. *EMBO Rep*. 2010;11(12):969-976.
6. Zotti T, Uva A, Ferravante A, et al. TRAF7 protein promotes Lys-29-linked polyubiquitination of IkappaB kinase (IKKgamma)/NF-kappaB essential modulator (NEMO) and p65/RelA protein and represses NF-kappaB activation. *J Biol Chem*. 2011;286(26):22924-22933.
7. Wang L, Wang L, Zhang S, et al. Downregulation of ubiquitin E3 ligase TNF receptor-associated factor 7 leads to stabilization of p53 in breast cancer. *Oncol Rep*. 2013;29(1):283-287.
8. Morita Y, Kanei-Ishii C, Nomura T, Ishii S. TRAF7 sequesters c-Myb to the cytoplasm by stimulating its sumoylation. *Mol Biol Cell*. 2005;16(11):5433-5444.
9. Shirakura K, Ishiba R, Kashio T, et al. The Robo4-TRAF7 complex suppresses endothelial hyperpermeability in inflammation. *J Cell Sci*. 2019;132(1).
10. Clark VE, Erson-Omay EZ, Serin A, et al. Genomic analysis of non-NF2 meningiomas reveals mutations in TRAF7, KLF4, AKT1, and SMO. *Science*. 2013;339(6123):1077-1080.
11. Clark VE, Harmancı AS, Bai H, et al. Recurrent somatic mutations in POLR2A define a distinct subset of meningiomas. *Nat Genet*. 2016;48(10):1253-1259.
12. Reuss DE, Piro RM, Jones DTW, et al. Secretory meningiomas are defined by combined KLF4 K409Q and TRAF7 mutations. *Acta Neuropathol*. 2013;125(3):351-358.
13. Abedalthagafi M, Bi WL, Aizer AA, et al. Oncogenic PI3K mutations are as common as AKT1 and SMO mutations in meningioma. *Neuro-oncology*. 2016;18(5):649-655.
14. Bueno R, Stawiski EW, Goldstein LD, et al. Comprehensive genomic analysis of malignant pleural mesothelioma identifies recurrent mutations, gene fusions and splicing alterations. *Nat Genet*. 2016;48(4):407-416.
15. Klein CJ, Wu Y, Jentoft ME, et al. Genomic analysis reveals frequent TRAF7 mutations in intraneural perineuriomas. *Ann Neurol*. 2017;81(2):316-321.
16. Goode B, Joseph NM, Stevers M, et al. Adenomatoid tumors of the male and female genital tract are defined by TRAF7 mutations that drive aberrant NF-kB pathway activation. *Mod Pathol*. 2018;31(4):660-673.
17. Stevers M, Rabban JT, Garg K, et al. Well-differentiated papillary mesothelioma of the peritoneum is genetically defined by mutually exclusive mutations in TRAF7 and CDC42. *Mod Pathol*. 2019;32(1):88-99.
18. Tokita MJ, Chen C-A, Chitayat D, et al. De Novo Missense Variants in TRAF7 Cause Developmental Delay, Congenital Anomalies, and Dysmorphic Features. *Am J Hum Genet*. 2018;103(1):154-162.
19. Adzhubei IA, Schmidt S, Peshkin L, et al. A method and server for predicting damaging

missense mutations. *Nat Methods*. 2010;7(4):248-249.
20. Sobreira N, Schiettecatte F, Valle D, Hamosh A. GeneMatcher: a matching tool for connecting investigators with an interest in the same gene. *Hum Mutat*. 2015;36(10):928-930.
21. Firth HV, Richards SM, Bevan AP, et al. DECIPHER: Database of Chromosomal Imbalance and Phenotype in Humans Using Ensembl Resources. *Am J Hum Genet*. 2009;84(4):524-533.
22. Lessel D, Kubisch C. Hereditary Syndromes with Signs of Premature Aging. *Dtsch Arztebl Int*. 2019;116(29-30):489-496.
23. Verloes A, Bremond-Gignac D, Isidor B, et al. Blepharophimosis-mental retardation (BMR) syndromes: A proposed clinical classification of the so-called Ohdo syndrome, and delineation of two new BMR syndromes, one X-linked and one autosomal recessive. *Am J Med Genet A*. 2006;140(12):1285-1296.
24. Li J, Ma J, Wang KS, et al. Baicalein inhibits TNF-α-induced NF-κB activation and expression of NF-κB-regulated target gene products. *Oncol Rep*. 2016;36(5):2771-2776.
25. Sharpe HJ, Pau G, Dijkgraaf GJ, et al. Genomic analysis of smoothened inhibitor resistance in basal cell carcinoma. *Cancer Cell*. 2015;27(3):327-341.
26. Schapira M, Tyers M, Torrent M, Arrowsmith CH. WD40 repeat domain proteins: a novel target class? *Nat Rev Drug Discov*. 2017;16(11):773-786.
27. Yang J, Boerm M, McCarty M, et al. Mekk3 is essential for early embryonic cardiovascular development. *Nat Genet*. 2000;24(3):309-313.
28. Newbern J, Zhong J, Wickramasinghe RS, et al. Mouse and human phenotypes indicate a critical conserved role for ERK2 signaling in neural crest development. *Proc Natl Acad Sci USA*. 2008;105(44):17115-17120.
29. Samuels IS, Karlo JC, Faruzzi AN, et al. Deletion of ERK2 mitogen-activated protein kinase identifies its key roles in cortical neurogenesis and cognitive function. *J Neurosci*. 2008;28(27):6983-6995.
30. Zhang Q, Lenardo MJ, Baltimore D. 30 Years of NF-κB: A Blossoming of Relevance to Human Pathobiology. *Cell*. 2017;168(1-2):37-57.
31. Sil AK, Maeda S, Sano Y, Roop DR, Karin M. IkappaB kinase-alpha acts in the epidermis to control skeletal and craniofacial morphogenesis. *Nature*. 2004;428(6983):660-664.
32. Park YC, Burkitt V, Villa AR, Tong L, Wu H. Structural basis for self-association and receptor recognition of human TRAF2. *Nature*. 1999;398(6727):533-538.
33. Yoshida H, Jono H, Kai H, Li J-D. The tumor suppressor cylindromatosis (CYLD) acts as a negative regulator for toll-like receptor 2 signaling via negative cross-talk with TRAF6 AND TRAF7. *J Biol Chem*. 2005;280(49):41111-41121.
34. Régnier CH, Masson R, Kedinger V, et al. Impaired neural tube closure, axial skeleton malformations, and tracheal ring disruption in TRAF4-deficient mice. *Proc Natl Acad Sci USA*. 2002;99(8):5585-5590.
35. Shiels H, Li X, Schumacker PT, et al. TRAF4 deficiency leads to tracheal malformation with resulting alterations in air flow to the lungs. *Am J Pathol*. 2000;157(2):679-688.
36. Krakow D, Robertson SP, King LM, et al. Mutations in the gene encoding filamin B disrupt vertebral segmentation, joint formation and skeletogenesis. *Nat Genet*. 2004;36(4):405-410.
37. Hooper AT, Shmelkov SV, Gupta S, et al. Angiomodulin is a specific marker of vasculature and regulates vascular endothelial growth factor-A-dependent neoangiogenesis. *Circ Res*. 2009;105(2):201-208.
38. Wolchinsky Z, Shivtiel S, Kouwenhoven EN, et al. Angiomodulin is required for

cardiogenesis of embryonic stem cells and is maintained by a feedback loop network of p63 and Activin-A. *Stem Cell Res*. 2014;12(1):49-59.
39. Abu-Safieh L, Abboud EB, Alkuraya H, et al. Mutation of IGFBP7 causes upregulation of BRAF/MEK/ERK pathway and familial retinal arterial macroaneurysms. *Am J Hum Genet*. 2011;89(2):313-319.
40. Domenga V, Fardoux P, Lacombe P, et al. Notch3 is required for arterial identity and maturation of vascular smooth muscle cells. *Genes Dev*. 2004;18(22):2730-2735.
41. Mašek J, Andersson ER. The developmental biology of genetic Notch disorders. *Development*. 2017;144(10):1743-1763.
42. Gripp KW, Robbins KM, Sobreira NL, et al. Truncating mutations in the last exon of NOTCH3 cause lateral meningocele syndrome. *Am J Med Genet A*. 2015;167A(2):271-281.
43. Delbridge ARD, Grabow S, Strasser A, Vaux DL. Thirty years of BCL-2: translating cell death discoveries into novel cancer therapies. *Nat Rev Cancer*. 2016;16(2):99-109.
44. Smith WL, Garavito RM, DeWitt DL. Prostaglandin endoperoxide H synthases (cyclooxygenases)-1 and -2. *J Biol Chem*. 1996;271(52):33157-33160.
45. Loftin CD, Trivedi DB, Tiano HF, et al. Failure of ductus arteriosus closure and remodeling in neonatal mice deficient in cyclooxygenase-1 and cyclooxygenase-2. *Proc Natl Acad Sci USA*. 2001;98(3):1059-1064.
46. Suri C, Jones PF, Patan S, et al. Requisite role of angiopoietin-1, a ligand for the TIE2 receptor, during embryonic angiogenesis. *Cell*. 1996;87(7):1171-1180.
47. Jeansson M, Gawlik A, Anderson G, et al. Angiopoietin-1 is essential in mouse vasculature during development and in response to injury. *J Clin Invest*. 2011;121(6):2278-2289.
48. Kim KH, Nakaoka Y, Augustin HG, Koh GY. Myocardial Angiopoietin-1 Controls Atrial Chamber Morphogenesis by Spatiotemporal Degradation of Cardiac Jelly. *Cell Rep*. 2018;23(8):2455-2466.
49. Yamaguchi TP, Bradley A, McMahon AP, Jones S. A Wnt5a pathway underlies outgrowth of multiple structures in the vertebrate embryo. *Development*. 1999;126(6):1211-1223.
50. Roifman M, Marcelis CLM, Paton T, et al. De novo WNT5A-associated autosomal dominant Robinow syndrome suggests specificity of genotype and phenotype. *Clin Genet*. 2015;87(1):34-41.
51. Uchiyama Y, Sakaguchi M, Terabayashi T, et al. Kif26b, a kinesin family gene, regulates adhesion of the embryonic kidney mesenchyme. *Proc Natl Acad Sci USA*. 2010;107(20):9240-9245.
52. Susman MW, Karuna EP, Kunz RC, et al. Kinesin superfamily protein Kif26b links Wnt5a-Ror signaling to the control of cell and tissue behaviors in vertebrates. *Elife*. 2017;6.
53. Najm J, Horn D, Wimplinger I, et al. Mutations of CASK cause an X-linked brain malformation phenotype with microcephaly and hypoplasia of the brainstem and cerebellum. *Nat Genet*. 2008;40(9):1065-1067.
54. Campos-Xavier AB, Martinet D, Bateman J, et al. Mutations in the heparan-sulfate proteoglycan glypican 6 (GPC6) impair endochondral ossification and cause recessive omodysplasia. *Am J Hum Genet*. 2009;84(6):760-770.
55. James MJ, Järvinen E, Thesleff I. Bono1: a gene associated with regions of deposition of bone and dentine. *Gene Expr Patterns*. 2004;4(5):595-599.
56. Shibata Y, Tsukazaki T, Hirata K, Xin C, Yamaguchi A. Role of a new member of IGFBP superfamily, IGFBP-rP10, in proliferation and differentiation of osteoblastic cells. *Biochem Biophys Res Commun*. 2004;325(4):1194-1200.
57. Biesma DH, Hannema AJ, van Velzen-Blad H, et al. A family with complement factor D

deficiency. *J Clin Invest*. 2001;108(2):233-240.
58. Deciphering Developmental Disorders Study. Large-scale discovery of novel genetic causes of developmental disorders. *Nature*. 2015;519(7542):223-228.
59. Amendola LM, Berg JS, Horowitz CR, et al. The Clinical Sequencing Evidence-Generating Research Consortium: Integrating Genomic Sequencing in Diverse and Medically Underserved Populations. *Am J Hum Genet*. 2018;103(3):319-327.
60. Urreizti R, Roca-Ayats N, Trepat J, et al. Screening of CD96 and ASXL1 in 11 patients with Opitz C or Bohring-Opitz syndromes. *Am J Med Genet A*. 2016;170A(1):24-31.
61. Deciphering Developmental Disorders Study. Prevalence and architecture of de novo mutations in developmental disorders. *Nature*. 2017;542(7642):433-438.

Figure legends

Figure 1. TRAF7 variants. Domain boundaries drawn approximately to scale, based on ref[6]. Variants causing the *TRAF7* syndrome are indicated in red (reported here) or grey (previously reported[18]). In pink, variants of unknown significance reported here. Beneath the protein, the most recurrent somatic variants (ie, in greater than five samples) are indicated; in black, those reported in meningiomas[11,12] and in blue, those in adenomatoid tumors of the genital tract[16]. CC; coiled-coil.

Figure 2. Facial features of patients with variants in *TRAF7*. Patient numbers are indicated at the top of each panel. See text for description of the major features.

Figure 3. Anomalies of the extremities (A) and upper body appearance (B) of patients with variants in *TRAF7*. Patient numbers are indicated at the top of each panel. See text for description of the major features.

Figure 4. qRT-PCR quantification of mRNA levels in *TRAF7* syndrome patient fibroblasts. (A) qRT-PCR of *BCL2*, *PTGS2*, *IGFBP7*, *NOTCH3*, *TRAF7* and *FLNB* in fibroblasts from three patients, with or without TNFα treatment. Relative mRNA level was normalized to the mean of six controls in each treatment condition (dotted line). *GAPDH* was used as a reference gene (the use of *PPIA* gave similar results). Data shown represents the mean ± SEM of the three patients, in six independent experiments. Asterisks indicate significant differences ($p<0.05$) between patients and controls in the corresponding condition (treated or untreated). (B) qRT-PCR validation of DEGs identified by RNA-Seq: *ANGPT1*, *CASK*, *KIF26B*, *KRAS*, *RIT1*, *WNT5A*, *CFD*, *GPC6* and

KAZALD1. Relative mRNA level was normalized to the mean of six controls in each treatment condition (dotted line). *GAPDH* was used as a reference gene (the use of *PPIA* gave similar results). Data shown represents the mean ± SEM of the four patients, in two independent experiments. Asterisks indicate significant differences ($p<0.05$) between patients and controls in the corresponding condition (treated or untreated).

Figure 5. Transcriptome analysis of fibroblasts bearing missense *TRAF7* variants. (A) Volcano plots representing differentially expressed genes (DEGs) in each condition (untreated or treated with TNFα (10 ng/ml) for 6 hours), measuring changes in expression (log_2 fold change) and their significance (FDR; $-log_{10}$ adjusted p-value). (B) Proportions of up- and down-regulated transcripts in untreated or treated patient fibroblasts. (C) Venn diagrams representing overlapping up- and down-regulated DEGs. (D and E) Ingenuity Pathway Analysis of DEGs in *TRAF7* syndrome patient fibroblasts. (D) Selected over-represented Canonical Pathways. The number of DEGs included in each pathway is specified and a $-log_{10}$ p-value >1.3 was considered significant. (E) Selected over-represented categories of "Cellular Functions and Physiological System Development". The number of DEGs associated with each category is specified and a $-log_{10}$ p-value >1.3 was considered significant.

Tables

Table 1. Top 10 up- and down-regulated genes identified in *TRAF7* syndrome patient fibroblasts by RNA-Seq.

Supplementary Figure legends

Supplementary Figure S1. Pedigree of the familial case (patients 24-26).

Supplementary Figure S2. *TRAF7* syndrome facial composite. The image was generated at Face2gene (https://www.face2gene.com) using one photo from each of 19 children with *TRAF7* syndrome.

Supplementary Figure S3. MTT viability assay. Fibroblasts from four patients and six controls were exposed to TNFα (10 ng/ml) for 24 hours or 48 hours. Data represent the relative cell viability (mean ± SD) of three independent experiments (in triplicate). Significant differences are indicated by * (p-value <0.05, One Way ANOVA test).

Supplementary Tables

Supplementary Table S1. Detailed clinical features of patients studied in this report. A phenotypic description of patient 33 has been previously published (patient P6 in ref[60]). The *TRAF7* variants of patients 6 and 8 were listed in ref[61], without phenotypic information. ABR=auditory brainstem response; CMA=chromosomal microarray analysis; EEG=electroencephalogram; GERD= gastroesophageal reflux disease; ID=intellectual disability; IPS=integrated prenatal screening; MEP=motor evoked potential; NA=not available; NAp=not applicable; ND=not done; PPV=positive pressure ventilation; SGA=small for gestational age; SSEP=somatosensory evoked potential; VEEG=video electroencephalogram; VER=visual evoked response; VUS=variant of unknown significance; ES=exome sequencing.

Supplementary Table S2. Characteristics of the *TRAF7* variants identified in the 43 index cases. [1]Parentheses around patients 1, 2 and 4 indicate that their variants should be considered of unknown significance. [2]cDNA coordinates refer to NM_032271.2.

Supplementary Table S3. Summary of phenotypes associated with *TRAF7* variants in the core cohort of 42 cases (patients 3 and 5-45). *, three patients born significantly prematurely are included within the total number of cases with patent ductus arteriosus.

Supplementary Table S4. Detailed list of DEGs identified in *TRAF7* syndrome patient fibroblasts by RNA-Seq. Only those DEGs with an adjusted p-value <0.05 and $|\log_2$ fold change$|$ in expression ≥1 are listed.

Supplementary Table S5. Genes selected for qPCR validation. T = transcriptomic criteria, i.e., high differential expression in the RNA-Seq data; F = functional criteria, i.e., for most, alteration in a relevant human disease or animal model. Note that *KRAS*, *SPTAN1*, *CASK*, *MAPK11* and *RIT1* did not meet the $\log_2$ fold change threshold for inclusion in the detailed DEG list in Supplementary Table S4.

Supplementary Table S6. Complete list of significant IPA pathways and functions. Categories are ordered according to their p-values. A cutoff of 0.05 was chosen.

Supplementary Table S7. Undiagnosed Diseases Network members list.

Disclosure

M.T.C. and S.Y. are employees of GeneDx, Inc.

Figure1

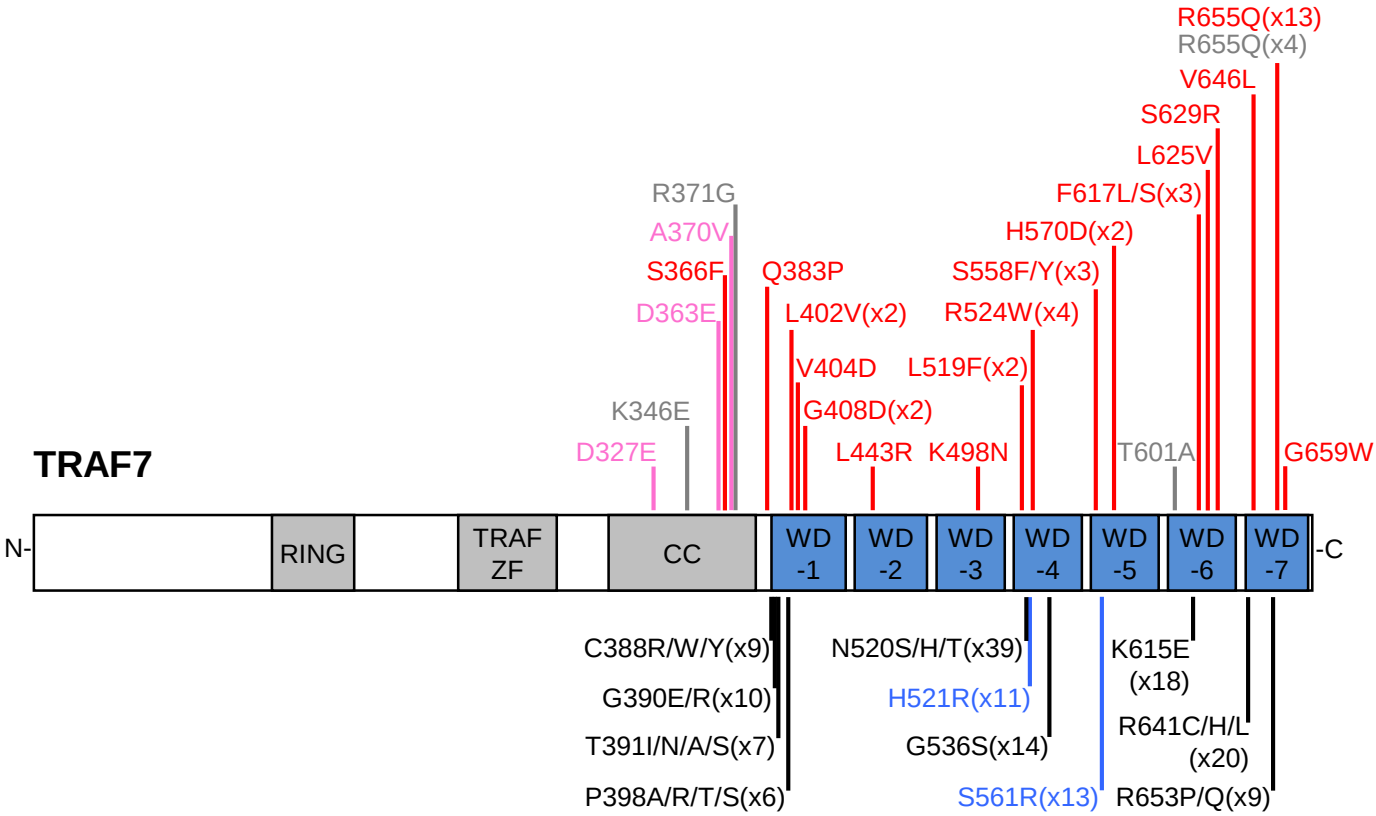
TRAF7
N-
RING
TRAF ZF
CC
WD -1
WD -2
WD -3
WD -4
WD -5
WD -6
WD -7
-C
R655Q(x13)
R655Q(x4)
V646L
S629R
L625V
F617L/S(x3)
H570D(x2)
S558F/Y(x3)
R524W(x4)
L519F(x2)
T601A
G659W
K498N
L443R
G408D(x2)
V404D
L402V(x2)
Q383P
R371G
A370V
S366F
D363E
K346E
D327E
C388R/W/Y(x9)
G390E/R(x10)
T391I/N/A/S(x7)
P398A/R/T/S(x6)
N520S/H/T(x39)
H521R(x11)
G536S(x14)
S561R(x13)
K615E (x18)
R641C/H/L (x20)
R653P/Q(x9)

Figure2

Figure3

Figure4

Click here to access/download;Figure;Figure 4 v3.tif

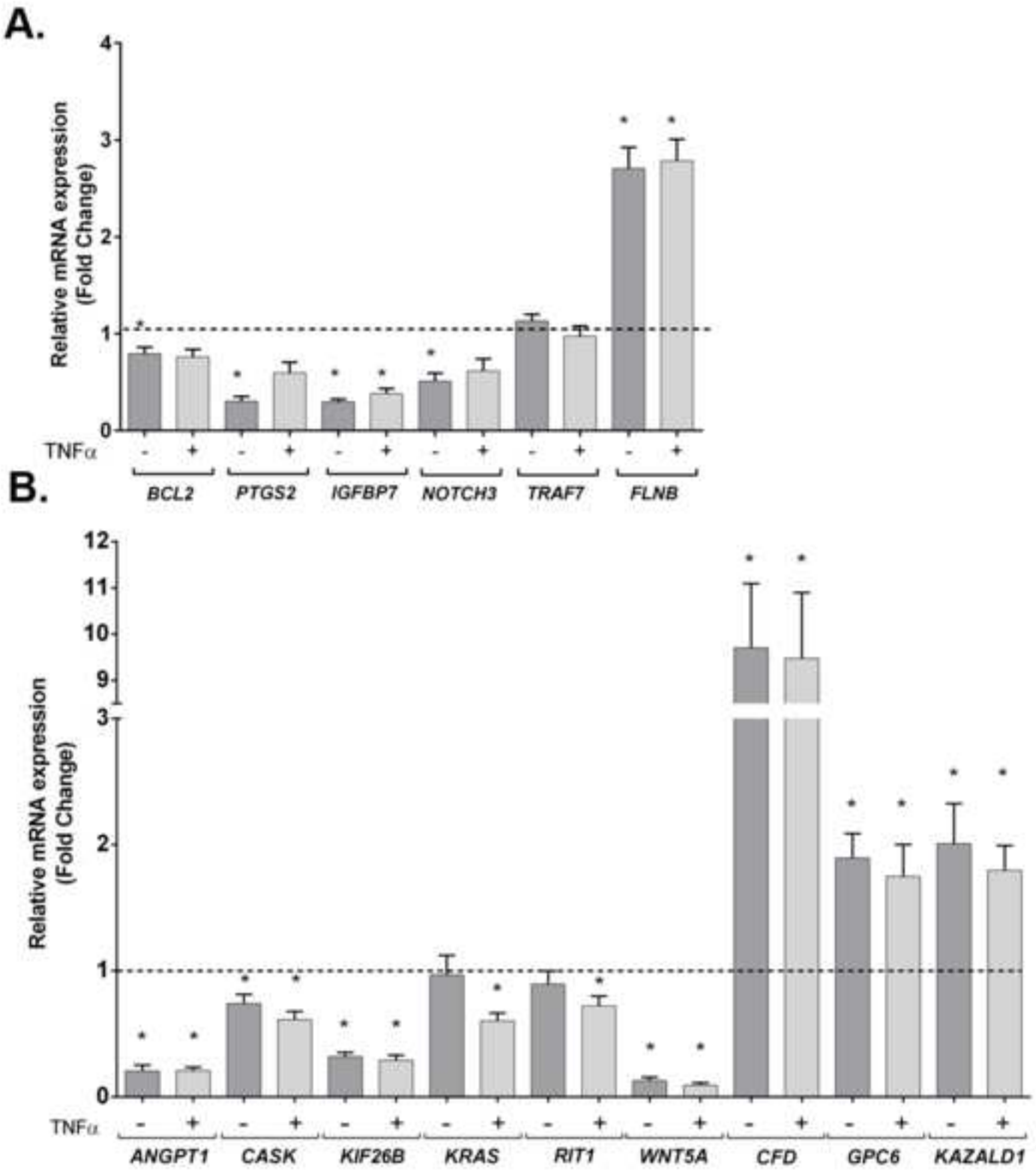

Figure5

Click here to access/download;Figure;Figure 5 v2.tif

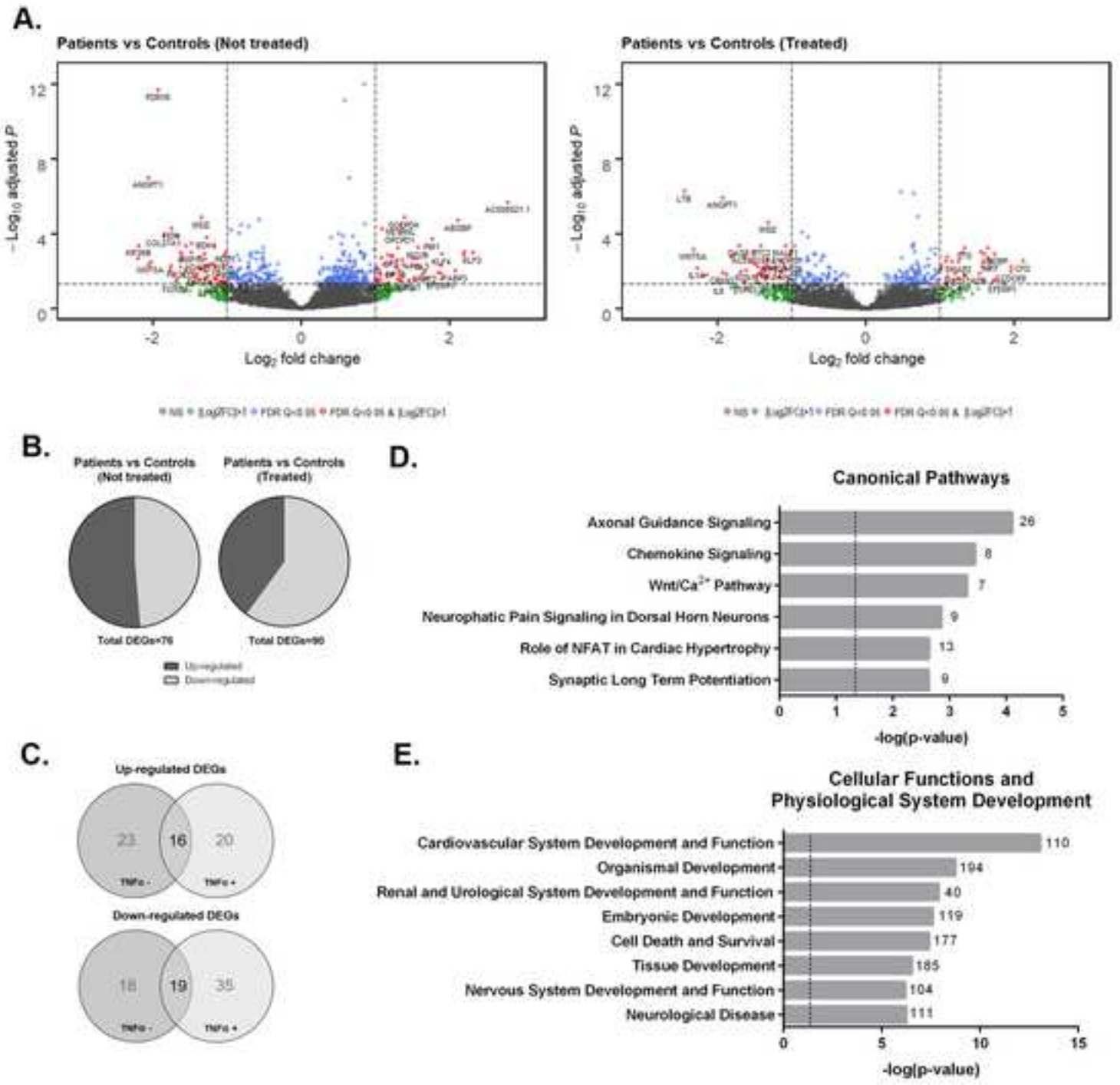

Table 1. Top 10 up- and down-regulated genes identified in *TRAF7* syndrome patient fibroblasts by RNA-Seq

	- TNFα				+ TNFα		
	Gene	**Log_2FC**	**FC**	**FDR**	**Gene**	**Log_2FC**	**FC**	**FDR**
Up-regulated	*PCOLCE2*	2.20	4.60	9.76E-04	*CFD*	2.12	4.34	2.89E-03
	CFD	2.19	4.56	1.34E-03	*CCDC69*	1.96	3.89	1.00E-02
	ABI3BP	2.11	4.31	1.98E-05	*PCOLCE2*	1.96	3.88	5.86E-03
	KLF4	1.90	3.74	1.26E-03	*EFEMP1*	1.85	3.59	4.07E-02
	ACKR3	1.89	3.71	4.74E-03	*DMKN*	1.77	3.41	3.18E-02
	DMKN	1.89	3.71	1.40E-02	*ABI3BP*	1.74	3.33	1.21E-03
	GPC6	1.85	3.60	1.24E-02	*GPC6*	1.72	3.30	3.01E-02
	PIM1	1.77	3.41	2.00E-04	*SYPL2*	1.70	3.25	3.91E-02
	RARRES3	1.64	3.11	3.19E-02	*MITF*	1.68	3.21	3.10E-03
	RHOB	1.64	3.11	1.52E-02	*TCF7*	1.67	3.17	8.02E-03
Down-regulated	*KIF26B*	-2.20	0.22	4.32E-04	*LTB*	-2.45	0.18	5.57E-07
	ANGPT1	-2.07	0.24	9.95E-08	*WNT5A*	-2.32	0.20	6.98E-04
	WNT5A	-2.04	0.24	3.42E-03	*IL1A*	-2.28	0.21	6.99E-03
	P2RX6	-1.94	0.26	2.11E-12	*NR4A2*	-2.21	0.22	1.82E-02
	COL27A1	-1.85	0.28	1.35E-04	*GNA14*	-2.14	0.23	1.56E-02
	IFI6	-1.77	0.29	8.49E-03	*IL6*	-1.98	0.25	4.59E-02
	FIGN	-1.75	0.30	5.31E-05	*ANGPT1*	-1.94	0.26	1.22E-06
	TRIM16L	-1.64	0.32	1.07E-03	*CPXM2*	-1.93	0.26	1.28E-02
	PIK3CD	-1.63	0.32	6.06E-03	*LRRN3*	-1.88	0.27	1.51E-02
	TLE4	-1.62	0.33	2.61E-03	*CYR61*	-1.82	0.28	1.78E-03

FigureS1

TRAF7; NM_032271.2; c.1851C>G; p.Phe617Leu

* whole exome sequencing

Affected individuals: 24, 25, 26

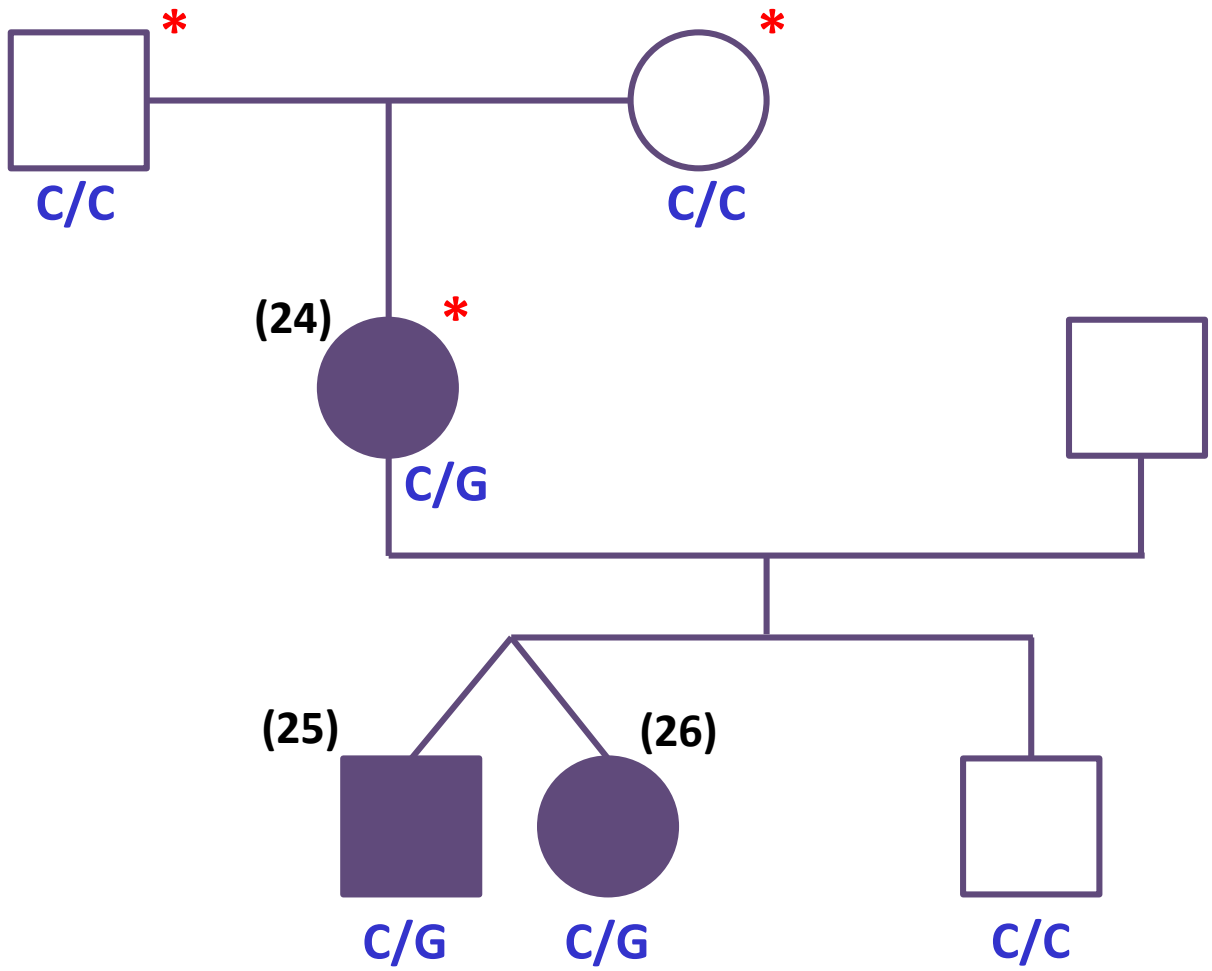

FigureS2

Click here to access/download;Supplementary (Appendix, online only material, etc.);Figure S2 - TRAF7 Face2Gene composite.png

FigureS3

Click here to access/download;Supplementary (Appendix, online only material, etc.);Figure S3 - MTT assay v2.tif

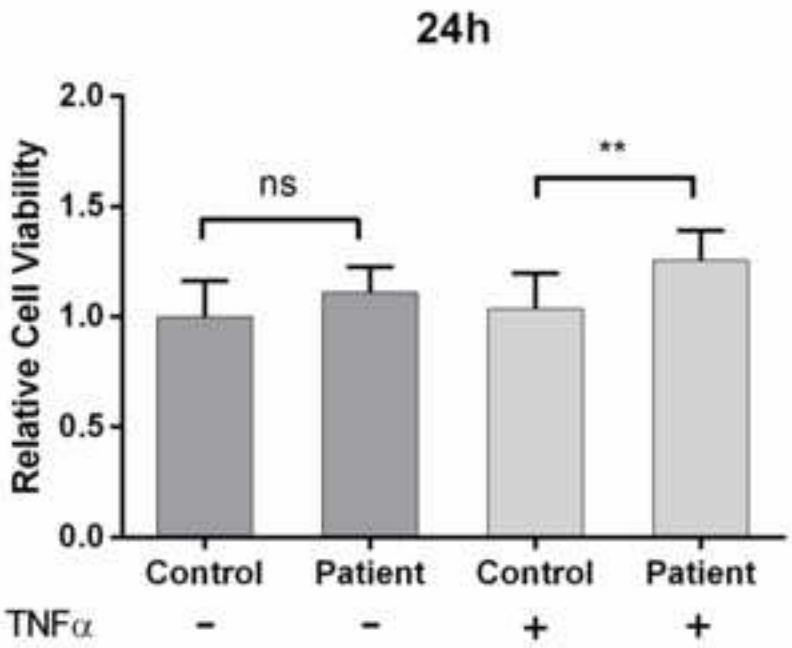

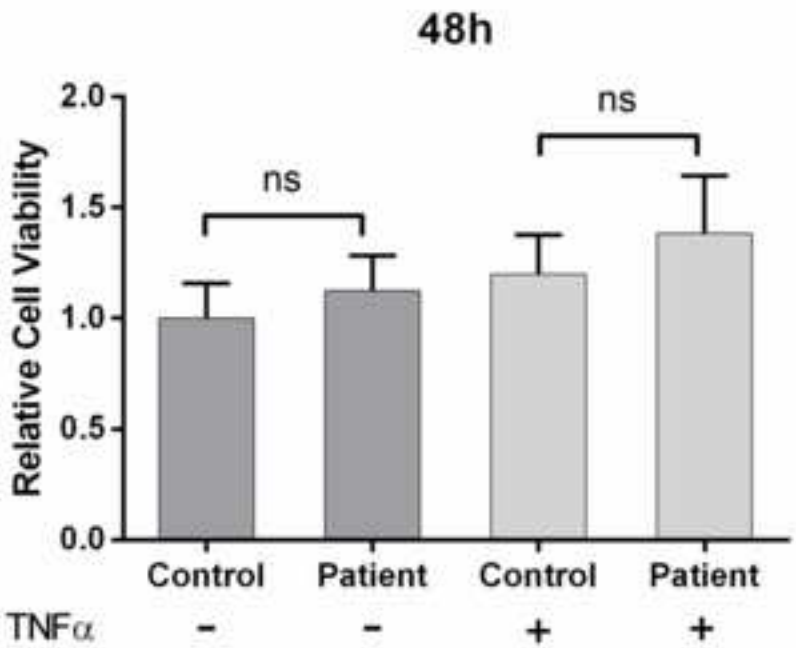

Supplementary Table S5. Genes selected for qPCR validation.

		- TNFα			+ TNFα				
Gene	**Ensembl Gene ID**	**Log_2FC**	**FC**	**FDR**	**Log_2FC**	**FC**	**FDR**	**Validated**	**Selection Criteria**
CFD	*ENSG00000197766*	2.19	4.56	1.34E-03	2.12	4.34	2.89E-03	Yes	T
GPC6	*ENSG00000183098*	1.85	3.6	1.24E-02	1.72	3.3	3.01E-02	Yes	T/F
KAZALD1	*ENSG00000107821*	1.24	2.36	1.50E-02	1.64	3.12	6.09E-04	Yes	T
FOXP1	*ENSG00000114861*	1.02	2.03	7.08E-03	-	-	-	No	F
KRAS	*ENSG00000133703*	0.85	1.8	1.07E-12	0.64	1.56	7.22E-07	No	F
SPTAN1	*ENSG00000197694*	0.51	1.43	3.67E-02	-	-	-	No	F
KIF26B	*ENSG00000162849*	-2.2	0.22	4.32E-04	-	-	-	Yes	T
ANGPT1	*ENSG00000154188*	-2.07	0.24	9.95E-08	-1.94	0.26	1.22E-06	Yes	T
WNT5A	*ENSG00000114251*	-2.04	0.24	3.42E-03	-2.32	0.2	6.98E-04	Yes	T
CASK	*ENSG00000147044*	-	-	-	-0.84	0.56	3.12E-02	Yes	F
MAPK11	*ENSG00000185386*	-0.68	0.62	1.02E-03	-0.69	0.62	1.21E-03	No	F
RIT1	*ENSG00000143622*	-0.49	0.71	4.41E-02	-	-	-	No	F

Members of the Undiagnosed Diseases Network

Maria T. Acosta
Margaret Adam
David R. Adams
Pankaj B. Agrawal
Mercedes E. Alejandro
Justin Alvey
Laura Amendola
Ashley Andrews
Euan A. Ashley
Mahshid S. Azamian
Carlos A. Bacino
Guney Bademci
Eva Baker
Ashok Balasubramanyam
Dustin Baldridge
Jim Bale
Michael Bamshad
Jordan Barham
Deborah Barbouth
Gabriel F. Batzli
Pinar Bayrak-Toydemir
Anita Beck
Alan H. Beggs
Gill Bejerano
Hugo J. Bellen
Jimmy Bennet
Beverly Berg-Rood
Raphael Bernier
Jonathan A. Bernstein
Gerard T. Berry
Anna Bican
Stephanie Bivona
Elizabeth Blue
John Bohnsack
Carsten Bonnenmann
Devon Bonner
Lorenzo Botto
Brenna Boyd
Lauren C. Briere
Elly Brokamp
Gabrielle Brown
Elizabeth A. Burke
Lindsay C. Burrage
Manish J. Butte
Peter Byers
William E. Byrd
John Carey
Olveen Carrasquillo
Ta Chen Peter Chang

Sirisak Chanprasert
Hsiao-Tuan Chao
Mei-Jan Chen
Gary D. Clark
Terra R. Coakley
Laurel A. Cobban
Joy D. Cogan
F. Sessions Cole
Heather A. Colley
Cynthia M. Cooper
Heidi Cope
William J. Craigen
Michael Cunningham
Precilla D'Souza
Hongzheng Dai
Surendra Dasari
Mariska Davids
Jyoti G. Dayal
Esteban C. Dell'Angelica
Shweta U. Dhar
Katrina Dipple
Daniel Doherty
Naghmeh Dorrani
Emilie D. Douine
David D. Draper
Laura Duncan
Dawn Earl
David J. Eckstein
Lisa T. Emrick
Christine M. Eng
Cecilia Esteves
Tyra Estwick
Liliana Fernandez
Carlos Ferreira
Elizabeth L. Fieg
Paul G. Fisher
Brent L. Fogel
Irman Forghani
Laure Fresard
William A. Gahl
Ian Glass
Rena A. Godfrey
Katie Golden-Grant
Alica M. Goldman
David B. Goldstein
Alana Grajewski
Catherine A. Groden
Andrea L. Gropman
Sihoun Hahn
Rizwan Hamid
Neil A. Hanchard

Nichole Hayes
Frances High
Anne Hing
Fuki M. Hisama
Ingrid A. Holm
Jason Hom
Martha Horike-Pyne
Alden Huang
Yong Huang
Rosario Isasi
Fariha Jamal
Gail P. Jarvik
Jeffrey Jarvik
Suman Jayadev
Jean M. Johnston
Lefkothea Karaviti
Emily G. Kelley
Dana Kiley
Isaac S. Kohane
Jennefer N. Kohler
Deborah Krakow
Donna M. Krasnewich
Susan Korrick
Mary Koziura
Joel B. Krier
Seema R. Lalani
Byron Lam
Christina Lam
Brendan C. Lanpher
Ian R. Lanza
C. Christopher Lau
Kimberly LeBlanc
Brendan H. Lee
Hane Lee
Roy Levitt
Richard A. Lewis
Sharyn A. Lincoln
Pengfei Liu
Xue Zhong Liu
Nicola Longo
Sandra K. Loo
Joseph Loscalzo
Richard L. Maas
Ellen F. Macnamara
Calum A. MacRae
Valerie V. Maduro
Marta M. Majcherska
May Christine V. Malicdan
Laura A. Mamounas
Teri A. Manolio
Rong Mao

Kenneth Maravilla
Thomas C. Markello
Ronit Marom
Gabor Marth
Beth A. Martin
Martin G. Martin
Julian A. Martínez-Agosto
Shruti Marwaha
Jacob McCauley
Allyn McConkie-Rosell
Colleen E. McCormack
Alexa T. McCray
Elisabeth McGee
Heather Mefford
J. Lawrence Merritt
Matthew Might
Ghayda Mirzaa
Eva Morava-Kozicz
Paolo M. Moretti
Marie Morimoto
John J. Mulvihill
David R. Murdock
Mariko Nakano-Okuno
Avi Nath
Stan F. Nelson
John H. Newman
Sarah K. Nicholas
Deborah Nickerson
Donna Novacic
Devin Oglesbee
James P. Orengo
Laura Pace
Stephen Pak
J. Carl Pallais
Christina GS. Palmer
Jeanette C. Papp
Neil H. Parker
John A. Phillips III
Jennifer E. Posey
John H. Postlethwait
Lorraine Potocki
Barbara N. Pusey
Aaron Quinlan
Wendy Raskind
Archana N. Raja
Genecee Renteria
Chloe M. Reuter
Lynette Rives
Amy K. Robertson
Lance H. Rodan
Jill A. Rosenfeld

Natalie Rosenwasser
Robb K. Rowley
Maura Ruzhnikov
Ralph Sacco
Jacinda B. Sampson
Susan L. Samson
Mario Saporta
C. Ron Scott
Judy Schaechter
Timothy Schedl
Kelly Schoch
Daryl A. Scott
Lisa Shakachite
Prashant Sharma
Vandana Shashi
Jimann Shin
Rebecca Signer
Catherine H. Sillari
Edwin K. Silverman
Janet S. Sinsheimer
Kathy Sisco
Edward C. Smith
Kevin S. Smith
Lilianna Solnica-Krezel
Rebecca C. Spillmann
Joan M. Stoler
Nicholas Stong
Jennifer A. Sullivan
Angela Sun
Shirley Sutton
David A. Sweetser
Virginia Sybert
Holly K. Tabor
Cecelia P. Tamburro
Queenie K.-G. Tan
Mustafa Tekin
Fred Telischi
Willa Thorson
Cynthia J. Tifft
Camilo Toro
Alyssa A. Tran
Tiina K. Urv
Matt Velinder
Dave Viskochil
Tiphanie P. Vogel
Colleen E. Wahl
Stephanie Wallace
Nicole M. Walley
Chris A. Walsh
Melissa Walker
Jennifer Wambach

Jijun Wan
Lee-kai Wang
Michael F. Wangler
Patricia A. Ward
Daniel Wegner
Mark Wener
Tara Wenger
Katherine Wesseling Perry
Monte Westerfield
Matthew T. Wheeler
Anastasia L. Wise
Lynne A. Wolfe
Jeremy D. Woods
Shinya Yamamoto
John Yang
Guoyun Yu
Diane B. Zastrow
Chunli Zhao
Stephan Zuchner

TableS1

Click here to access/download

Large Excel File

Table S1 - phenotype details V5_clean.xlsx

TableS2

Click here to access/download

Large Excel File

Table S2 - mutation details V3.xlsx

TableS3

Click here to access/download

Large Excel File

Table S3 - phenotype summary V4.xlsx

TableS4

Click here to access/download

Large Excel File

Table S4 - List of DEGs.xlsx

Click here to access/download

Large Excel File

Table S6 - Enriched IPA Pathways and Functions.xlsx